

Probing the Kinetics of Short-Distance Drug Release from Nanocarriers to Nanoacceptors**

Hong Wang, Jun Xu, Jinghao Wang, Tao Chen, Yong Wang, Yan Wen Tan, Haibin Su, Khai Leok Chan, and Hongyu Chen*

Targeted delivery and controlled release of a drug to specific organs or cells would potentially maximize its therapeutic efficacy while minimizing the side effects. This is of particular importance for insoluble drugs, as there is a lack of means to transport them in a biological system. Many insoluble drug candidates failed clinical trials because of poor pharmacokinetics. With an effective delivery system, these drugs could be reexplored to unleash their potential. So far, a variety of micro- and nanoscale materials have been developed as drug carriers.^[1] Of paramount significance for biological application is an understanding of the pathway and the rate of drug release from these new materials.

A model system for the study of kinetics entails the delivery of a model drug, typically an organic dye, from a carrier to an acceptor through a solvent. In contrast to the focus on nanocarriers, though, few systems in the literature included nanoscale acceptors to model biological acceptors such as proteins and lipid membranes. A practical concern is the lack of means to distinguish the drug molecules in carriers from those in acceptors. Dialysis-based methods separated nanocarriers from water by a semipermeable membrane, so the drug content on each side could be analyzed by methods such as UV/Vis spectroscopy,^[2] fluorescence,^[3] or chromatography.^[4] Alternatively, a bulk organic phase was used to extract the released drug in water away from the nanocarriers.^[5] In these examples, the released drug molecules have to diffuse through a bulk phase (water and/or an organic solvent) before being characterized. In a different approach, paramagnetic ions (Ti³⁺)^[5d] were used to quench the fluorescence of released drug, and Au nanoparticles (NPs) were used as quenchers for the loaded drugs in nanocarriers.^[5c] Thus, the

fluorescence change of the model drugs in the different media (solvent versus carriers) allowed real-time monitoring of the drug release without disrupting the delivery system.

For drug release in a cellular environment, the nanocarriers would be intimately mixed with the nanoscale bioacceptors. Hence, short-distance diffusion (ca. 1 μm) would dominate, and the use of bulk-phase acceptors could not fully mimic this process. Recently, an enlightening work by Chen et al. used dual-labeled polymer micelles as nanocarriers,^[6] so that the drug release could be studied in the presence of nanoacceptors.

Herein, we report a new model delivery system, in which pyrene was incorporated in the polymer shells of AuNPs and then released to nanoacceptors (Figure 1). The fluorescence of pyrene was quenched in the vicinity of the AuNPs but

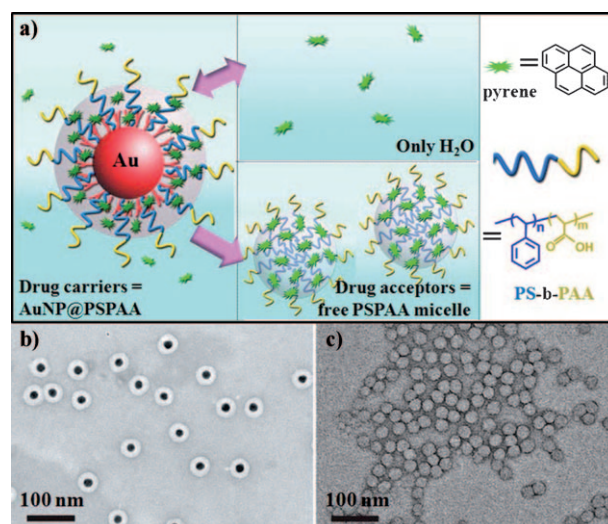


Figure 1. A new kinetics model for drug release. a) Release of pyrene from the polymer shells of AuNPs: in the absence of nanoacceptors, the system quickly reaches equilibrium without significant material transfer; in the presence of excess free PSPAA micelles, the short-distance transfer of pyrene is fast. b,c) Transmission electron microscopy (TEM) images of pyrene-loaded AuNP@PSPAA (b) and free PSPAA micelles (c).

reemerged upon its release, thus allowing in situ kinetics study by optical measurements. To mimic cell components, bovine serum albumin (BSA), L- α -phosphatidylcholine (a phospholipid) micelles, sodium dodecyl sulfate (SDS) micelles, and polystyrene-*block*-poly(acrylic acid) (PSPAA) micelles were used as nanoacceptors. The intimate mixing of the nanocarriers with the nanoacceptors creates a realistic model for

[*] H. Wang, J. Xu, T. Chen, Y. Wang, Y. W. Tan, Prof. H. Chen
Division of Chemistry and Biological Chemistry
Nanyang Technological University
21 Nanyang Link, Singapore 637371 (Singapore)
Fax: (+65) 6791-1961
E-mail: hongyuchen@ntu.edu.sg
Homepage: <http://www.ntu.edu.sg/home/hongyuchen/>
J. Wang, Prof. H. Su
School of Materials Science and Engineering
Nanyang Technological University, Singapore 639798 (Singapore)
Dr. K. L. Chan
Institute of Materials Research and Engineering (IMRE) and the
Agency for Science, Technology, and Research (A*STAR)
Singapore 117602 (Singapore)

[**] We thank the Ministry of Education, Singapore (ARC 13/09) for financial support.

Supporting information for this article is available on the WWW under <http://dx.doi.org/10.1002/anie.201001065>.

short-distance drug release. Using pyrene as a limiting model for hydrophobic drugs, the critical role of nanoacceptors in the kinetics of drug release was demonstrated.

To prepare drug carriers, AuNPs were encapsulated by PSPAA shells (AuNP@PSPAA, Figure 1b) following previously reported methods.^[7] The uniform micellar shells on AuNPs are similar in nature to empty micelles of PSPAA (Figure 1c), which have been shown to incorporate hydrophobic molecules such as pyrene.^[8] Pyrene could be directly loaded in AuNP@PSPAA during the AuNP encapsulation,^[9] but an alternative method was used here that is compatible with other molecular payloads. Pyrene was transferred from “free” PSPAA micelles (with no AuNPs) to AuNP@PSPAA. It was first incubated with PSPAA in a DMF-rich solvent ($V_{\text{H}_2\text{O}}/V_{\text{DMF}} = 2:1$); its enhanced solubility in this solution indicated its incorporation in the polymer micelles. Purified AuNP@PSPAA ($d_{\text{Au}} = (16 \pm 1.8) \text{ nm}$; $d_{\text{overall}} = (43 \pm 2.6) \text{ nm}$) were then added and the mixture was incubated at 80 °C for 4 hours. The concentration of pyrene in the free PSPAA micelles was higher than that in the AuNP@PSPAA, and this concentration gradient drove the transfer of pyrene to the AuNP@PSPAA. The high DMF content of the solution swelled the polymer micelles, thus facilitating the equilibration of pyrene in the system.

After pyrene incorporation, the heavy AuNP@PSPAA were readily isolated by centrifugation, and the product was diluted with water to reduce the DMF content, thus deswelling the PSPAA micelles and trapping pyrene inside. In the collected solution of pyrene-loaded AuNP@PSPAA, there were still small amounts of residual DMF and free PSPAA micelles. To completely remove these impurities, the concentrated samples (ca. 10 μL) were diluted with NaOH (0.1 mM, 1.5 mL) and further purified by centrifugation (typically five cycles in total). The NaOH solution was used to increase the charge repulsion and minimize the aggregation of AuNP@PSPAA during the multiple steps of centrifugation.^[10a]

TEM characterization of the resulting AuNP@PSPAA (Figure 1b) showed that they were structurally identical to those before pyrene incorporation. In particular, there was no apparent change in the thickness of the polymer shells. UV/Vis spectra of the sample after each cycle of purification showed the characteristic absorption peaks of pyrene at 323 and 339 nm, and the plasmon absorption peak of AuNPs at 530 nm (Figure 2a). The fact that pyrene was co-separated with the AuNP@PSPAA strongly supported its residence in the polymer shells.

The fluorescence signal of pyrene is affected by three main factors. AuNPs have strong absorbance at 200–600 nm, and it attenuates both the excitation beam and the fluorescence signal (inner filter effect). Although metal NPs quench the fluorescence of pyrene at close proximity, molecules at a distance from the Au surface could be enhanced by surface-enhanced fluorescence (SEF).^[11] In kinetics experiments, the fluorescence intensity was measured in situ with an invariant AuNP concentration. Thus, the inner filter effect reduces all signals by a constant ratio. Furthermore, pyrene was probably distributed uniformly inside the polymer shells, and thus the combined effects of quenching and SEF affected the fluores-

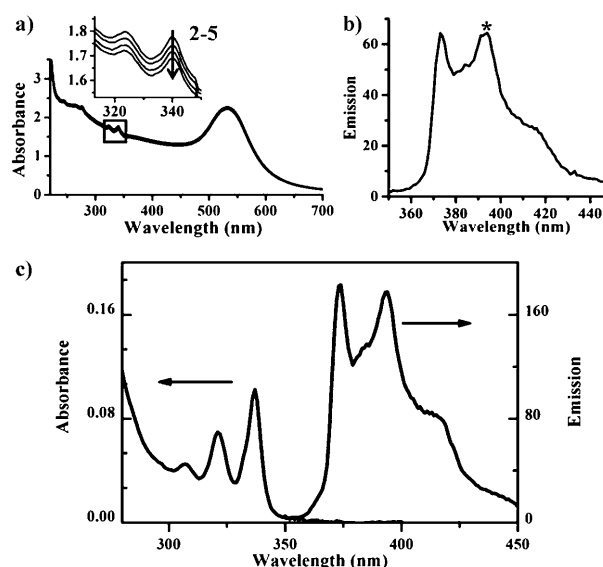


Figure 2. Evidence for the loading of pyrene in AuNP@PSPAA. a) UV/Vis absorption spectra of the pyrene-impregnated AuNP@PSPAA in water after five cycles of purification; lines 2–5 (inset) are for samples after the respective centrifugation cycle. b) Emission spectrum of pyrene-loaded AuNP@PSPAA in water (* indicates the emission peak at 395 nm that was followed in all kinetic traces). c) Absorption and emission spectra of the released pyrene, after disassembling the pyrene-loaded AuNP@PSPAA in DMF and removing the AuNPs.

cence signals in proportion to the number of incorporated pyrene molecules. Since the signal of pyrene-loaded AuNP@PSPAA (Figure 2b) was weaker than that of the same sample after release (63 versus 215), SEF should be less significant than the quenching effect.

Nevertheless, these factors make it difficult to quantify the incorporated pyrene. To overcome this problem, the pyrene-loaded AuNP@PSPAA were disassembled in a hot DMF solution: the polymer shells were dissolved and the stripped AuNPs were removed by centrifugation. The resulting solution showed pyrene absorption peaks at 307, 323, and 339 nm, and emission peaks at 373, 384, 395, and 415 nm (Figure 2c). The fluorescence of pyrene was not used, as it is different in water and DMF. Based on UV/Vis spectra of standard samples, pyrene in this solution was quantified. It was further estimated that there was an average 2019 ± 42 pyrene molecules per AuNP@PSPAA, which is equivalent to about 0.06 molecules/nm³ in the polymer shell.^[9]

In an aqueous solution and in the absence of nanoacceptors, pyrene is stable in AuNP@PSPAA. The fluorescence of the loaded nanocarriers in 2 mL water did not show any obvious change in 2 hours (Figure 3a). The minimal pyrene release could be attributed to its very low solubility in water ($7 \times 10^{-7} \text{ M}$) and also to the lack of organic solvent (e.g., DMF) to swell the polymer shells. While the former limits the pyrene release thermodynamically, the latter controls the rate of release kinetically. The slow release allowed the purification of the pyrene-loaded AuNP@PSPAA without losing a significant amount of the payload.

With the development and characterization of nanocarriers, the next step is to find suitable nanoacceptors. A

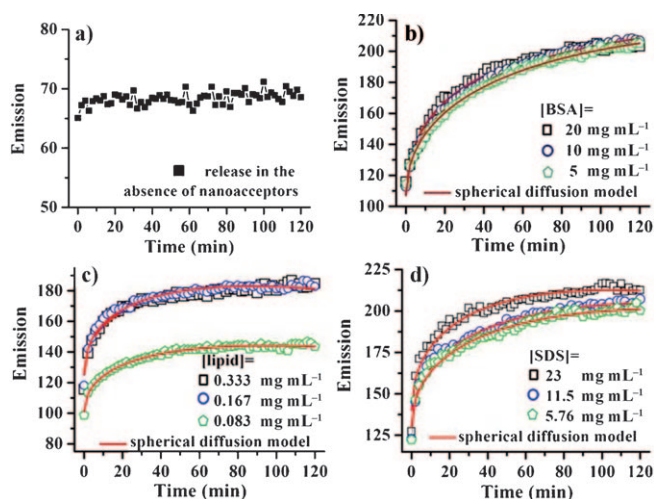


Figure 3. Nanoacceptor-assisted pyrene release. a) Fluorescence intensity trace (at 395 nm) of pyrene-loaded AuNP@PSPAA upon incubation in water. b–d) Fluorescence intensity traces showing the kinetics of pyrene release when BSA, L- α -phosphatidylcholine micelles, and SDS micelles, respectively, were used as nanoacceptors; the red lines were fitted to the Fickian diffusion model.

biological system is abundant in nanoacceptors such as proteins and cell membranes, which could readily take up hydrophobic molecules by recognition, adsorption, or simple dissolution. Hence, the drug transfer among the various hosts could be nonspecific and difficult to study, particularly with the unknown concentrations of the bioacceptors. In a model system, we were able to introduce nanoacceptors in known concentrations, so that the drug release kinetics could be studied in detail. BSA is the main plasma protein in bovine blood circulation, and it is known to absorb hydrophobic molecules such as pyrene.^[12] Thus, it represents a general protein that could recognize or absorb a specific drug.

In a kinetic experiment, BSA was added to a solution of pyrene-loaded AuNP@PSPAA in water, so that the nanoacceptors were homogeneously mixed with the nanocarriers. As pyrene dissociated from the AuNP@PSPAA, its fluorescence intensity increased because of the increased distance from pyrene to an Au surface. Therefore, the concentration of the released pyrene is directly related to the fluorescence intensity, thus allowing in situ and real-time monitoring of the drug release by fluorescence measurement. Fast increase of the pyrene emission at 395 nm was observed (Figure 3b). Based on the fluorescence intensity, over 60% of the incorporated pyrene was released within 2 hours.

In addition to BSA, we also used micelles of small molecules to mimic cell membranes, which are primarily made of proteins and lipids. L- α -Phosphatidylcholine is a type of naturally occurring lipid. We prepared micelles of this molecule by following literature procedures,^[13a] and then added them to an aqueous solution of pyrene-loaded AuNP@PSPAA. As shown in Figure 3c, the release of pyrene was also fast. A similar result was obtained when SDS micelles were used as the nanoacceptors (Figure 3d). The similarity in the kinetic behavior of the drug release when

three different nanoacceptors were used (Figure 3b–d) is a strong indication for a common mechanism.

However, exactly how pyrene was transferred from the nanocarriers to the nanoacceptors is still unknown. There are at least three different possible pathways. Pyrene could be first released to the aqueous phase and then diffuse into the nanoacceptors, or it could be directly transferred when a transient bridge is formed between a nanocarrier and a nanoacceptor during their collision. The latter scenario was previously suggested to explain the fast drug transfer in the presence of nanoacceptors.^[6] Alternatively, the micelles of nanocarriers and nanoacceptors could dynamically disassemble and re-form in solution, thus facilitating material transfer among them. This is particularly likely when the nanoacceptors are made of small molecules such as BSA, SDS, and lipid, which are known to rapidly dissolve and re-form in aqueous solution.

In contrast to the dynamic behavior of small-molecule micelles, PSPAA micelles have been shown to be kinetically frozen with low liquidity.^[13b] A vivid demonstration can be found in our recent report,^[10d] in which hollow PSPAA micelles were shown to maintain their structure in aqueous solution until they were heated beyond the glass transition temperature of polystyrene. Thus, under the conditions of our experiments, the PSPAA molecules in the micelles could not exchange and the micelles could not split or fuse with each other. Moreover, it is known that the PSPAA micelles are highly charged and do not aggregate even in saturated CsCl solutions.^[10a–c] Given the long PAA chains (ca. 60 acrylic acid repeating units) on the surface of the micelles, it is unlikely that hydrophobic channels could form between two micelles during a collision. Therefore, the use of PSPAA in both nanocarriers and nanoacceptors minimizes the mechanistic ambiguities.

To prepare empty PSPAA micelles as nanoacceptors, PSPAA was heated in a H₂O/DMF (4.5:1, v/v) mixture to induce its self-assembly; the resulting free micelles (Figure 1c, $d = (24 \pm 3.0)$ nm) were diluted with water and further dialyzed against water to completely remove DMF. Then, the pyrene-loaded AuNP@PSPAA were added to this solution to initiate the drug transfer. A fast increase of emission intensity at 395 nm was observed (Figure 4a), which indicated the efficient release of pyrene. In this system, the free PSPAA micelles were in large excess to the AuNP@PSPAA and the ratio was estimated to be 149:1 in number of particles ([free micelle] = 0.4 mg mL⁻¹).^[9] On average, each AuNP@PSPAA occupies a cube of width 1.5 μ m with these acceptors. Hence, the distance of pyrene diffusion in water should be in the range of a few hundred nanometers, and the fast Brownian motion of both the nanocarriers and the nanoacceptors is expected to facilitate pyrene transfer.

Since the average diffusion distance between nanocarriers and nanoacceptors is determined by their concentrations, the kinetic experiments were carried out at varying concentrations of the nanoacceptors. In Figure 4a, the rate of pyrene release barely changed when the concentration of free PSPAA micelles changed from 0.4 to 0.2 (not shown) and 0.1 mg mL⁻¹, thus indicating that the “perfect sink” condition was attained for the pyrene released from nanocarriers. The

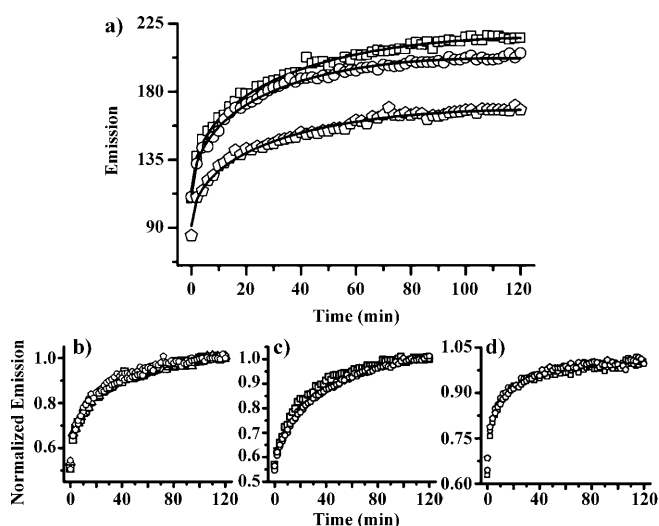


Figure 4. Understanding the kinetics of pyrene release. a) Fluorescence intensity traces showing the kinetics of pyrene release when free PSPAA micelles were used as nanoacceptors; [free micelle] (in mg mL^{-1}): \square 0.4; \circ 0.1; \diamond 0.05. The solid lines were fitted to the Fickian diffusion model. b–d) Normalized traces in (a), Figure 3 b, and Figure 3 c, respectively. b) [Free micelle] (in mg mL^{-1}): \square 0.4; \triangle 0.2; \circ 0.1; \diamond 0.05. c) [BSA] (in mg mL^{-1}): \square 20; \circ 10; \diamond 5. d) [Lipid] (in mg mL^{-1}): \square 0.333; \circ 0.167; \diamond 0.083.

“perfect sink” refers to the condition where excess acceptors are present for absorbing the released drug. In cases where no acceptor is used, it could also mean that the solubilizing capacity of the solvent is significantly greater than that of the released drug. However, further reducing the concentration of nanoacceptors (to 0.05 mg mL^{-1}) led to a lower plateau of emission intensity (Figure 4a). This can be attributed to the reduced amount of pyrene released at equilibrium (10 h)^[9] because of the lack of acceptors. The level of decrease in the fluorescence intensity at the plateau is also consistent with the decrease in the estimated volume ratio of nanocarriers to nanoacceptors,^[9] which supports the attainment of equilibrium at the end of pyrene release.

Importantly, after normalization, the four traces with different nanoacceptor concentrations exactly overlapped each other (Figure 4b). Since the average distance from AuNP@PSPAA to free PSPAA micelles changed in these experiments, this observation indicated that the diffusion of pyrene through water was not the rate-determining step. The same conclusions can be reached when other types of nanoacceptors are used (Figure 4c,d). Therefore, the kinetic model of our system is virtually equivalent to the direct diffusion of pyrene from AuNP@PSPAA to the surrounding nanoacceptors. Indeed, the fluorescence intensity traces of pyrene in Figures 3 and 4 fit well to the Fickian diffusion model^[14] (correlation coefficient $R > 0.98$) [Eq. (1)]:

$$Y = P_1 + P_2 t^{1/2} - P_3 t \quad (1)$$

where Y is the fluorescence intensity, which is proportional to the concentration of the released pyrene, t is time, and P_1 , P_2 , and P_3 are coefficients (values are given in Table S3 in the Supporting Information). The Fickian diffusion model was

previously used to describe the diffusion-controlled release of a substance from a sphere, assuming a constant diffusion coefficient. It best describes purely radial diffusion in the initial ($< 70\%$) release stage. The fact that all of our data fit well to this simple diffusion model supports a common mechanism when the diffusion of pyrene through water is efficient.

Therefore, the use of nanoscale acceptors has an important consequence on the kinetics of drug release. By removing the released pyrene from the aqueous phase, the presence of nanoacceptors greatly enhanced the rate of release from the nanocarriers. Similar results have been observed in a recent report using dual-labeled polymer micelles as nanocarriers.^[6] Importantly, the short-distance diffusion of a hydrophobic molecule such as pyrene through an aqueous phase is actually *not* the rate-determining step. Thus, the release kinetics can be solely described by the radial diffusion through the hydrophobic phases of both the carriers and acceptors, which reduces mechanistic complexity. This feature is independent of the nature of the nanoacceptors, so long as there is excess of them around. But it is distinctively different from other model systems that involve drug diffusion through a bulk phase. Most hydrophobic drugs are conceivably more soluble than pyrene in an aqueous phase, and hence their diffusion through water is expected to be faster. The abundance of nanoscale bioacceptors in a cellular environment makes it imperative to include nanoacceptors in model delivery systems. Otherwise, the rate of drug release or diffusion could be misinterpreted. For example, drug molecules incorporated in a delivery vehicle could be quickly and nonspecifically lost to the bioacceptors in a cell, even though they may be stable in the vehicle in the absence of nanoacceptors.

In conclusion, we have developed a new kinetic system that allows the use of both nanocarriers and nanoacceptors. The intimate mixing of the two at the nanoscale realistically mimics drug delivery in a cellular environment. In the model system, the carrier/acceptor concentrations could be readily controlled and the drug transfer could be monitored in real time. Using this unique system, pyrene was shown to quickly transfer (ca. 2 h) from the nanocarriers to the nanoacceptors. This nanoacceptor-induced fast release of pyrene follows the Fickian spherical diffusion model, and could be explained by the short-distance diffusion of pyrene through water. For its low solubility in water, pyrene was used as a limiting model for hydrophobic drugs with higher solubility. Biologically relevant nanoacceptors, such as BSA and lipid micelles, were used in our delivery system to model bioacceptors. The use of PSPAA micelles as both nanocarriers and nanoacceptors provided unique advantages in understanding the pathway of pyrene release. We have presented evidence to show that pyrene probably did transfer through water and that the transfer was not assisted by dynamic reassembly or fusion splitting of the polymer micelles.

Received: February 22, 2010

Revised: May 14, 2010

Published online: July 7, 2010

Keywords: drug delivery · kinetics · micelles · nanoparticles · diffusion model

- [1] a) T. M. Allen, P. R. Cullis, *Science* **2004**, *303*, 1818–1822; b) J. Y. Chen, S. Y. Chen, X. R. Zhao, L. V. Kuznetsova, S. S. Wong, I. Ojima, *J. Am. Chem. Soc.* **2008**, *130*, 16778–16785; c) K. K. Coté, M. E. Belowich, M. Liong, M. W. Ambrogio, Y. A. Lau, H. A. Khatib, J. I. Zink, N. M. Khashab, J. F. Stoddart, *Nanoscale* **2009**, *1*, 16–39; d) S. Elodie, C. Stephanie, B. Muriel, R.-L. Isabelle, *Angew. Chem.* **2009**, *121*, 280–295; *Angew. Chem. Int. Ed.* **2009**, *48*, 274–288; e) L. A. L. Satish Nayak, *Angew. Chem.* **2005**, *117*, 7862–7886; *Angew. Chem. Int. Ed.* **2005**, *44*, 7686–7708; f) A. H. Tamsyn, M. H. James, *Small* **2009**, *5*, 300–308; g) T. T. Morgan, H. S. Muddana, E. I. Altinoglu, S. M. Rouse, A. Tabakovic, T. Tabouillot, T. J. Russin, S. S. Shanmugavelandy, P. J. Butler, P. C. Eklund, J. K. Yun, M. Kester, J. H. Adair, *Nano Lett.* **2008**, *8*, 4108–4115.
- [2] a) E. Aznar, M. D. Marcos, R. Martinez-Manez, F. Sancenon, J. Soto, P. Amoros, C. Guillem, *J. Am. Chem. Soc.* **2009**, *131*, 6833–6843; b) N. Nasongkla, E. Bey, J. M. Ren, H. Ai, C. Khemtong, J. S. Guthi, S. F. Chin, A. D. Sherry, D. A. Boothman, J. M. Gao, *Nano Lett.* **2006**, *6*, 2427–2430; c) R. Vyhnalkova, A. Eisenberg, T. G. M. van de Ven, *J. Phys. Chem. B* **2008**, *112*, 8477–8485; d) J. X. Zhang, P. X. Ma, *Angew. Chem.* **2009**, *121*, 982–986; *Angew. Chem. Int. Ed.* **2009**, *48*, 964–968.
- [3] a) P. L. Soo, L. B. Luo, D. Maysinger, A. Eisenberg, *Langmuir* **2002**, *18*, 9996–10004; b) J. Yang, C. H. Lee, J. Park, S. Seo, E. K. Lim, Y. J. Song, J. S. Suh, H. G. Yoon, Y. M. Huh, S. Haam, *J. Mater. Chem.* **2007**, *17*, 2695–2699.
- [4] A. P. Griset, J. Walpole, R. Liu, A. Gaffey, Y. L. Colson, M. W. Grinstaff, *J. Am. Chem. Soc.* **2009**, *131*, 2469–2471.
- [5] a) Y. Cheng, A. C. Samia, J. D. Meyers, I. Panagopoulos, B. W. Fei, C. Burda, *J. Am. Chem. Soc.* **2008**, *130*, 10643–10647; b) R. Hong, G. Han, J. M. Fernandez, B. J. Kim, N. S. Forbes, V. M. Rotello, *J. Am. Chem. Soc.* **2006**, *128*, 1078–1079; c) C. K. Kim, P. Ghosh, C. Pagliuca, Z. J. Zhu, S. Menichetti, V. M. Rotello, *J. Am. Chem. Soc.* **2009**, *131*, 1360–1361; d) Y. Teng, M. E. Morrison, P. Munk, S. E. Webber, K. Prochazka, *Macromolecules* **1998**, *31*, 3578–3587.
- [6] H. T. Chen, S. W. Kim, L. Li, S. Y. Wang, K. Park, J. X. Cheng, *Proc. Natl. Acad. Sci. USA* **2008**, *105*, 6596–6601.
- [7] a) H. Chen, S. Abraham, J. Mendenhall, S. C. Delamarre, K. Smith, I. Kim, C. A. Batt, *ChemPhysChem* **2008**, *9*, 388–392; b) Y. J. Kang, T. A. Taton, *Angew. Chem.* **2005**, *117*, 413–416; *Angew. Chem. Int. Ed.* **2005**, *44*, 409–412; c) M. X. Yang, T. Chen, W. S. Lau, Y. Wang, Q. H. Tang, Y. H. Yang, H. Chen, *Small* **2009**, *5*, 198–202.
- [8] J. X. Zhao, C. Allen, A. Eisenberg, *Macromolecules* **1997**, *30*, 7143–7150.
- [9] See the Supporting Information for details.
- [10] a) G. Chen, Y. Wang, L. H. Tan, M. X. Yang, L. S. Tan, Y. Chen, H. Chen, *J. Am. Chem. Soc.* **2009**, *131*, 4218–4219; b) G. Chen, Y. Wang, M. Yang, J. Xu, S. J. Goh, M. Pan, H. Chen, *J. Am. Chem. Soc.* **2010**, *132*, 3644–3645; c) X. J. Wang, G. P. Li, T. Chen, M. X. Yang, Z. Zhang, T. Wu, H. Chen, *Nano Lett.* **2008**, *8*, 2643–2647; d) L. H. Tan, S. Xing, T. Chen, G. Chen, X. Huang, H. Zhang, H. Chen, *ACS Nano* **2009**, *3*, 3469–3474.
- [11] C. D. Geddes, K. Aslan, I. Gryczynski, J. Malicka, J. R. Lakowicz, *Rev. Fluoresc.* **2004**, *1*, 365–401.
- [12] a) R. K. Chowdhary, I. Shariff, D. Dolphin, *J. Pharm. Pharm. Sci.* **2003**, *6*, 13–19; b) E. N. Savariar, S. Ghosh, D. C. Gonzalez, S. Thayumanavan, *J. Am. Chem. Soc.* **2008**, *130*, 5416–5417.
- [13] a) G. Adhikary, S. Chandra, R. Sikdar, P. C. Sen, *Colloids Surf. B* **1995**, *4*, 335–339; b) M. Moffitt, K. Khogaz, A. Eisenberg, *Acc. Chem. Res.* **1996**, *29*, 95–102.
- [14] P. L. Ritger, N. A. Peppas, *J. Controlled Release* **1987**, *5*, 23–36.